Dynamic Resolution of Photocurrent Generating Pathways by Field-Dependent Ultrafast Microscopy

Kyle Vogt[1], **Sufei Shi**[2,3], **Feng Wang**[3] **and Matt W. Graham**[1]

[1.]*Department of Physics, Oregon State University, Corvallis, OR 97331, USA*
[2.]*Department of Chemical Engineering, Rensselaer Polytechnic Institute, Troy 12180, NY USA*
[3.]*Department of Physics, University of California, Berkeley 94720, CA USA*

graham@physics.oregonstate.edu

Abstract: Combining *E*-field-dependent ultrafast photocurrent and transient absorption microscopy, we develop a novel measurement to extract the rates determining photocurrent efficiency. For WSe$_2$, both techniques yield the same dissociation rate dependence.

OCIS codes: 320.7100 Ultrafast measurements, 320.7130 Ultrafast processes in condensed matter.

For most nanoscale materials, photoexcited electrons recombine at a time, τ_r which is far faster than electron-hole pair dissociation and escape times [1], $\tau_{d,e}$, resulting in inherently poor photocurrent generation efficiency given by, $\varepsilon \cong \frac{1/\tau_{d,e}}{1/\tau_d,e+1/\tau_r}$. Presently, there exists no reliable *in-situ* time-resolved method that selectively isolates both the $1/\tau_r$ and $1/\tau_d,e$ rates. Transport based measurements lack the required time resolution, while purely optical measurements give a convoluted weighted-average of all electronic dynamics, offering no selectivity for photocurrent generating pathways. Recently, the ultrafast photocurrent (U-PC) autocorrelation method has successfully measured the rate limiting electronic relaxation processes in materials such as graphene [2], carbon nanotubes [3], and transition metal dichalcogenide (TMD) materials [4]. Unfortunately, there still exists no standard response function to understand this U-PC response. Here, we derive and experimentally confirm a generic U-PC response function by simultaneously resolving the transient absorption (TA) and U-PC response for highly-efficient WSe$_2$ devices (depicted in Fig. 1a). For the first time, we show both optical TA and electrical U-PC responses give the same *E*-field-dependent electronic escape and recombination rates. We further show these rates quantify a material's intrinsic PC generation efficiency.
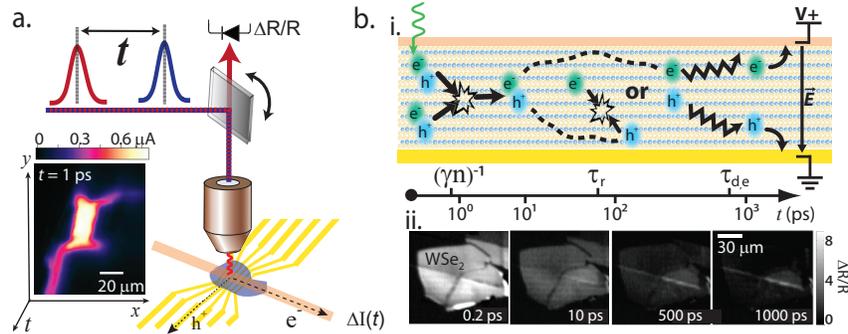
Fig. 1. *Experimental setup and timeline for charge extraction.* **(a)** In the WSe$_2$ device shown, we measure the exciton dissociation dynamics with U-PC, $\Delta I(t,V)$ and TA, $\Delta R(t,V)$. (*inset*) $t = 1$ ps scanning U-PC spatial map. **(b)** *i.* Cutaway of device geometry, with transparent top gate held at voltage V. It depicts a timeline of photocurrent generation events. *ii.* Scanning TA microscopy maps of few-layer WSe$_2$ show electron recombination.

We began by fabricating photoconductive (PC) devices of WSe$_2$, a van der Waals layered TMD. Such TMDs have recently attracted great interest owing to their large absorption cross-section, and the just discovered valley-Hall effect, enabling chiral light photosensitive detection [6,7]. PC is collected from devices that sandwich exfoliated WSe$_2$ between optically thin gold capacitive plates, as shown in Fig. 1a-b. Under applied bias, we resonantly excite the K/K' transitions with 120 fs pulses in confocal-scanning geometry, and find remarkably efficient electron extraction approaching 52%. Fig 1b depicts the complete timeline of the dominant photocurrent generating pathway we observe in WSe$_2$; from light absorption to photocurrent collection. The mechanism illustrated was determined by a novel

simultaneous measurement of both TA and U-PC responses (Fig. 2) that demonstrate we can selectively isolate the PC-relevant kinetic rates. Namely, the exciton-exciton annihilation ($\gamma n(t)$), recombination ($1/\tau_r$), electric field assisted dissociation and escape rate, $1/\tau_{d,e}$.
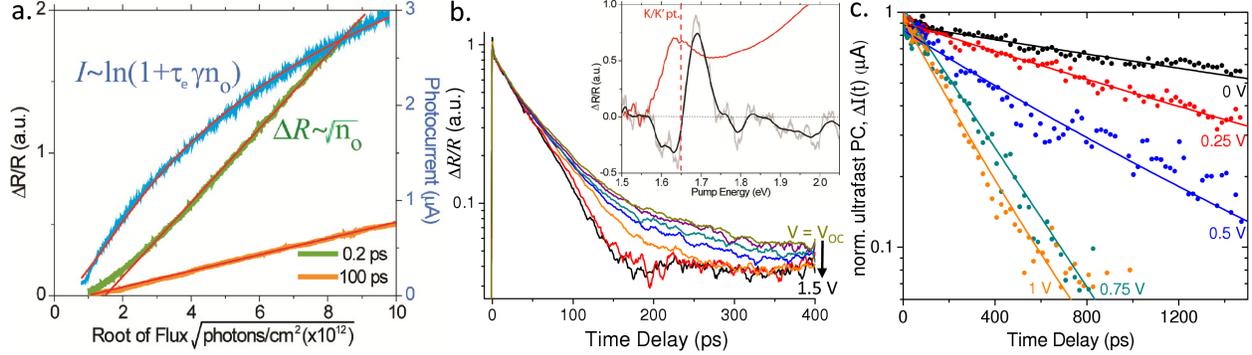
Fig. 2. *Annihilation and the U-PC response function.* **(a)** TA (green, orange) amplitude vs. square root of photon flux fits to a linear trend. PC (blue) instead fits to time-integrated response of $n(t)$. **(b)** WSe$_2$ TA kinetic decay accelerates with biases ranging from 0 to 1.5 V. (*inset*) Linear (*red*) and t=0.2 ps TA (*black*) spectrum of the WSe$_2$ photoconductive device. **(c)** Normalized U-PC response in WSe$_2$ accelerates with increasing bias, as the electrons are extracted.

Unlike typical bulk photodectors, for few-layer van der Waals materials like WSe$_2$ and MoS$_2$, we found many-body electronic interactions, most notably exciton-exciton annihilation still dominate the ultrafast kinetics and the overall PC response; as demonstrated by the square root scaling of the $\Delta R/R$ TA signals plotted in Fig. 2a [8]. This scaling suggests the kinetic rate law associated with photocurrent generation is $\frac{dn}{dt} \cong \delta(t)n_o - \kappa_{tot}n - \gamma n^2$, with $\kappa_{tot} = 1/\tau_r + 1/\tau_{d,e}$. We verify this law is correct by first predicting how the photocurrent depends on the initial number of photoexcited carriers created, n_o. By integration, we obtain $I(n_o) \propto \int_o^\infty n(t)dt \propto \ln\left(1 + \frac{\gamma}{\kappa_{tot}}n_o\right)$. This predictive dependence fits the observed PC response in Fig. 2a (blue data with red line fit) far better than the ad-hoc power laws used elsewhere [3,4]. We can now extend this theory to predict the change in photocurrent, defined as the difference between the two-pulse U-PC response autocorrelation (obtained by simply integrating the total carrier density piecewise about the stage delay time t'), and twice the steady state current obtained from a single beam. This yields:

$$\Delta I(t) \propto \int_o^t n(t', n_o)dt' + \int_t^\infty n(t', n_o + n(t))dt' - 2\int_o^\infty n(t', n_o)dt' \tag{1}$$

As shown in Fig. 2c, this time-integrated U-PC ultrafast decay increases markedly with applied bias voltage, selectively measuring the electron-hole dissociation and escape rates. Fig. 3a clearly depicts some anti-correlation between the number of carriers left in the state 125 ps after excitation in the TA measurement, and the amount of photocurrent generated at each applied E-field. This suggests that we are able to optically observe carriers leaving the device. We also note here that this dependence is approximately symmetric about the open circuit voltage, but the data points used to extract the time constants correspond to the negative bias data for both TA and U-PC experiments. Using Eq. 1 (solid line fits), we extract the U-PC kinetic rate constant, $1/\tau_{d,e}$ as a function of applied bias. We find in Fig. 3b that this rate constant increases quadratically with the applied E-field. To independently verify our U-PC response function (Eq. 1), we compare the U-PC rates against the purely optical TA kinetics plotted in Fig. 2b. Strikingly, Fig. 3b shows that the E-field-dependent TA optical rates (open squares) agree with the rates obtained from our U-PC data (closed circles). Specifically, in Fig. 3b the E-field dependent rate components of the TA decay both match the amplitude of the U-PC rates, and increase quadratically with applied E-field (red dashed line fit to open squares). As a slight contrast to our PC-pathway selective U-PC technique, the K-point transient bleach kinetics in Fig. 2b are a summation of all electronic kinetic pathways in WSe$_2$. This additional kinetic information enables us to fit the E-field dependent dissociation escape time, and the field independent annihilation and recombination rates to confirm the dynamic photocurrent extraction pathway proposed in Fig. 1b*i*. Further, we claim our U-PC response function can provide the rate constants associated with photocurrent generation in any device exhibiting nonlinear PC response.

Once the PC-associated rate constants are extracted from U-PC and TA microscopy, the material's intrinsic (rate-limiting) photocurrent generation efficiency can be calculated. Specifically in Fig. 3b, we plot (blue squares) the
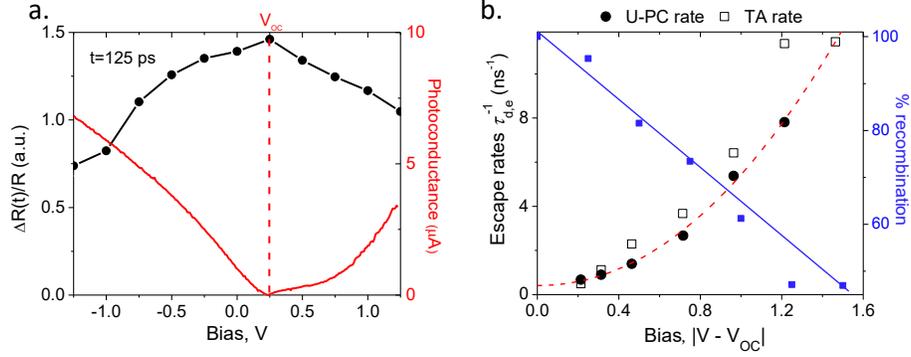
Fig. 3. *Correlated ultrafast PC and TA dissociation rates.* **(a)** About the open circuit voltage V_{OC}, PC and TA amplitude (at 125 ps) are anticorrelated with the applied ***E***-field. **(b)** U-PC electronic dissociation and escape times τ_{d}, e (circles) and those obtained from TA measurements (open squares) show the same quadratic dependence with applied ***E***-field. Calculated from associated rates, the blue squares plot $\%_{loss}$ of electrons lost due to recombination.

fraction of electrons lost to electron-hole recombination as obtained from the rate-calculated photocurrent efficiency, ε. We find the WSe$_2$ device intrinsic photocurrent efficiency increases linearly with applied field, to a maximum of ~52% efficiency. Ultimately, we find this TMD material's efficiency is limited by a field-independent electron-hole dissociation that occurs on the timescale of 87 ps, suggesting an inherent entropic barrier for charge dissociation. Additionally, this minimum time for charge extraction is less than that of recombination, 97 ps allowing for $\varepsilon > 50\%$.

In summary, few-layer semiconducting TMDs like WSe$_2$, have long carrier lifetimes, but challenging mobility and exciton dissociation bottlenecks that inhibit photocurrent generation. By combining E-field dependent ultrafast photocurrent with transient absorption microscopy [1,2,4,5], we have identified the dominant kinetic bottlenecks that inhibit photocurrent production in devices made from stacked few-layer TMD materials. Using our new ultrafast photocurrent response function, we show U-PC microscopy selectively resolves electron-hole dissociation and escape rates, providing a new methodology to intelligently select materials that intrinsically avoid recombination bottlenecks and maximize photocurrent yield.

[1] M.W. Graham, S. Shi, D.C. Ralph, J. Park, P.L. McEuen, "Transient Absorption and Photocurrent Microscopy Show That Hot Electron Supercollisions Describe the Rate-Limiting Relaxation Step in Graphene" Nano Letters, 13, 5497-5502 (2013).

[2] M.W. Graham, S. Shi, D.C. Ralph, J. Park, P.L. McEuen, "Photocurrent measurements of supercollision cooling in graphene," Nature Physics, 9, 103 (2013).

[3] N. M. Gabor, Z. Zhong, K. Bosnick, and P. L. McEuen, "Ultrafast Photocurrent Measurement of the Escape Time of Electrons and Holes from Carbon Nanotube p-i-n Photodiodes," Phys. Rev. Lett., 108, 8, 087404 (2012).

[4] M. Massicotte, P. Schmidt, F. Vialla, K. G. Schdler, A. Reserbat-Plantey, K. Watanabe, T. Taniguchi, K.-J. Tielrooij, and F. H. L. Koppens (2015), "Picosecond photodetection in vander Waals heterostructures," Nature Nanotech., 11, 42-46 (2015).

[5] H. Patel, R. Havener, L. Brown, Y. Liang, L. Yang, J. Park, M.W. Graham, "Tunable Optical Excitations in Twisted Bilayer Graphene Form Strongly Bound Excitons," Nano Letters, 15, 5932-7 (2015).

[6] H. Yuan, X. Wang, B. Lian, H. Zhang, X. Fang, B. Shen, G. Xu, Y. Xu, S.-C. Zhang, H. Y. Hwang, and Y. Cui, "Generation and electric control of spinvalley-coupled circular photogalvanic current in WSe$_2$," Nature Nano, 9, 851 (2014).

[7] K. F. Mak, K. L. McGill, J. Park, and P. L. McEuen, "The valley Hall effect in MoS$_2$ transistors," Science, 344, 1489 (2014).

[8] T. Borzda, C. Gadermaier, N. Vujicic, P. Topolovsek, M. Borovsak, T. Mertelj, D. Viola, C. Manzoni, E. A. A. Pogna, D. Brida, M. R. Antognazza, F. Scotognella, G. Lanzani, G. Cerullo, and D. Mihailovic, "Charge Photogeneration in Few-Layer MoS$_2$," Adv. Functional Materials, 25, 33513358 (2015).